

High resolution in-situ stable isotope measurements reveal atmospheric vapour dynamics above contrasting urban vegetation

Ann-Marie Ring¹, Dörthe Tetzlaff¹, Maren Dubbert², Dubbert D¹, and Chris Soulsby³

¹Leibniz-Institut für Gewässerökologie und Binnenfischerei im Forschungsverbund Berlin eV

²Leibniz-Zentrum für Agrarlandschaftsforschung (ZALF) e V

³University of Aberdeen School of Geosciences

May 5, 2023

Abstract

Quantitative knowledge about ecohydrological partitioning across the critical zone in different types of urban green space is important to balance sustainable water needs in cities during future challenges of increasing urbanization and climate warming. We monitored stable water isotopes in liquid precipitation and atmospheric water vapour (δ_v) using *in-situ* cavity ring-down spectroscopy (CRDS) over a two-month period in an urban green space area in Berlin, Germany. Our aim was to better understand the origins of atmospheric moisture and its link to water partitioning under contrasting urban vegetation. δ_v was monitored at multiple heights (0.15, 2 and 10 m) in grassland and forest plots. The isotopic composition of δ_v above both land uses was highly dynamic and positively correlated with that of rainfall indicating the changing sources of atmospheric moisture. Further, the isotopic composition of δ_v was similar across most heights of the 10 m profiles and between the two plots indicating limited aerodynamic mixing. Only the surface at ~0.15 m height above the grassland, δ_v showed significant differences, with more enriched values indicative of evaporative fractionation immediately after rainfall events. Further, disequilibrium between δ_v and precipitation composition was evident during and right after rainfall events with more positive values (i.e. vapour more enriched than precipitation) in summer and negative values in winter, which probably results from higher evapotranspiration and more convective precipitation events in summer. Our work showed that it is technically feasible to produce continuous, longer-term data on δ_v isotope composition in urban areas from *in-situ* monitoring using CRDS, providing novel insights into water cycling and partitioning across the critical zone of an urban green space. Such data has the potential to better constrain the isotopic interface between the atmosphere and the land surface and to improve ecohydrological models that can resolve evapotranspiration fluxes.

High resolution *in-situ* stable isotope measurements reveal atmospheric vapour dynamics above contrasting urban vegetation

Ring^{1,2}, Tetzlaff^{1,2,3}, Dubbert M⁴, Dubbert D^{1,4}, Soulsby³

¹ Department of Ecohydrology, Leibniz Institute of Freshwater Ecology and Inland Fisheries, Berlin, Germany.

² Department of Geography, Humboldt University Berlin, Berlin, Germany.

³ Northern Rivers Institute, School of Geosciences, University of Aberdeen, UK.

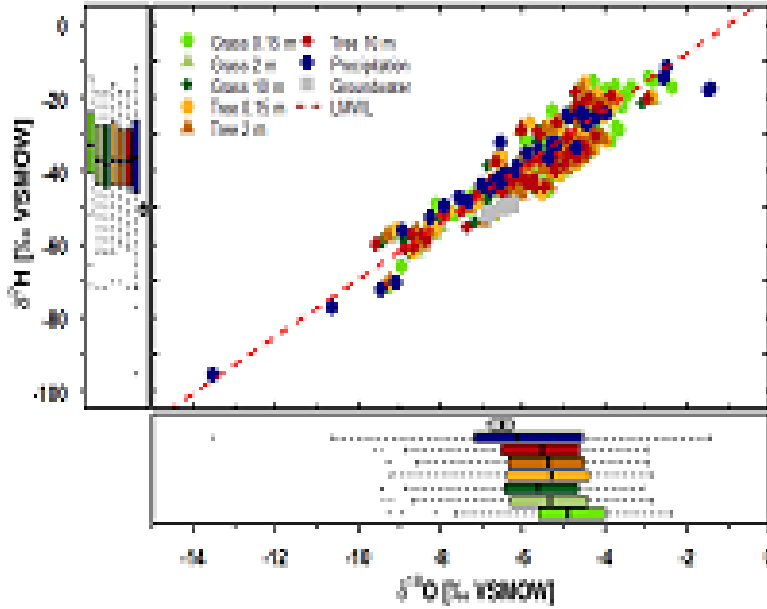
⁴ Research Area 1 “Landscape Processes”, Leibniz Institute for Agricultural and Landscape Research, Müncheberg, Germany

Corresponding author: Ann-Marie Ring (ann-marie.ring@igb-berlin.de); Doerthe Tetzlaff (doerthe.tetzlaff@igb-berlin.de)

Novelty and International Appeal Statement:

Quantitative knowledge about ecohydrological partitioning in different types of urban green space is important. We present novel high-resolution isotope data of atmospheric vapour (δ_v) measured continuously over several month in an urban green space. To our knowledge such data have not been measured in an urban green space setting with the goal to increase understanding evapotranspiration from different urban vegetation cover. We also detected occasional dis-equilibrium between vapour and precipitation isotopes.

Graphical Abstract Image:



Graphical Abstract Text:

High resolution *in-situ* stable isotope measurements reveal atmospheric vapour dynamics above contrasting urban vegetation

Ann-Marie Ring, Dörthe Tetzlaff, Maren Dubbert, David Dubbert, Chris Soulsby

In-situ measurements of urban atmospheric water isotopes (δ_v) at different elevations produce reliable high-resolution data. Urban atmospheric vapour is influenced by varying drivers depending on the type of green space. δ_v above grassland and tree stands was similar at 10 m height, but near-surface δ_v above indicated higher evaporation and vapour enrichment over grass. We detected occasional dis-equilibrium between vapour and precipitation isotopes.

Keywords: ecohydrology, urban green spaces, in-situ monitoring, atmospheric vapour isotopes, equilibrium assumption, cities

Main Findings

- *In-situ* measurements of urban atmospheric water isotopes (δ_v) at different elevations produce reliable high-resolution data.
- Urban atmospheric vapour is influenced by varying drivers depending on the type of green space.

- δ_v above grassland and tree stands was similar at 10 m height, but near-surface δ_v above indicated higher evaporation and vapour enrichment over grass.
- We detected occasional dis-equilibrium between vapour and precipitation isotopes.

Abstract

Quantitative knowledge about ecohydrological partitioning across the critical zone in different types of urban green space is important to balance sustainable water needs in cities during future challenges of increasing urbanization and climate warming. We monitored stable water isotopes in liquid precipitation and atmospheric water vapour (δ_v) using *in-situ* cavity ring-down spectroscopy (CRDS) over a two-month period in an urban green space area in Berlin, Germany. Our aim was to better understand the origins of atmospheric moisture and its link to water partitioning under contrasting urban vegetation. δ_v was monitored at multiple heights (0.15, 2 and 10 m) in grassland and forest plots. The isotopic composition of δ_v above both land uses was highly dynamic and positively correlated with that of rainfall indicating the changing sources of atmospheric moisture. Further, the isotopic composition of δ_v was similar across most heights of the 10 m profiles and between the two plots indicating limited aerodynamic mixing. Only the surface at ~ 0.15 m height above the grassland, δ_v showed significant differences, with more enriched values indicative of evaporative fractionation immediately after rainfall events. Further, disequilibrium between δ_v and precipitation composition was evident during and right after rainfall events with more positive values (i.e. vapour more enriched than precipitation) in summer and negative values in winter, which probably results from higher evapotranspiration and more convective precipitation events in summer. Our work showed that it is technically feasible to produce continuous, longer-term data on δ_v isotope composition in urban areas from *in-situ* monitoring using CRDS, providing novel insights into water cycling and partitioning across the critical zone of an urban green space. Such data has the potential to better constrain the isotopic interface between the atmosphere and the land surface and to improve ecohydrological models that can resolve evapotranspiration fluxes.

1. Introduction

Urban green spaces mediate trade-offs between “green” and “blue” water fluxes with potential for high evapotranspiration (ET) rates. They potentially mitigate the Urban Heat Island (UHI) effect, but on the other hand might reduce groundwater recharge and stream flow generation. Understanding, quantifying and optimizing this partitioning across urban critical zones is increasingly important in the face of increased urban growth and climatic warming. In addition, wider benefits of urban green spaces – or green infrastructure – are increasingly recognized; these include the potential to enhance infiltration and ameliorate urban storm runoff to increase local biodiversity, to provide social functions through improved health for local residents and to improve water security in terms of sufficient provision of good water quality. Consequently, as one component of an evidence base for wider urban planning, the trade-offs between higher ET rates and groundwater recharge, as well as the linked uncertainties, are an increased focus for research (e.g. BMUB).

Water stable isotopes have proved valuable tools that can help resolve the partitioning of incoming precipitation into different components of ET fluxes or to constrain biosphere-atmosphere feedbacks between atmospheric vapor and ET, and thus have high potential to contribute to a scientific evidence-base for managing urban green spaces. Water isotopes have also been shown to be a useful tracer to understand processes and linkages across the critical zone and the soil-plant-atmosphere continuum in different geographic regions although critical zone studies in urban areas are still relatively rare. Use of isotopes includes tracking the effects of evaporation in isotopic fractionation and in identifying the effects of seasonality of water sources for different vegetation types. Numerous isotope studies have used soil water or river water isotopes to assess evaporative effects, whilst others have related the composition of xylem water to potential sources of root water uptake. However, studies using high-resolution data to investigate how evaporation and/or transpiration affect the isotopic composition of atmospheric vapour (δ_v) at the surface boundary layer are especially rare for urban areas (e.g. Gorski et al.,).

The onset of relatively inexpensive cavity ring-down spectrometers (CRDS) has revolutionized the field of isotope studies allowing efficient tracing of isotopic transformations across the atmospheric water cycle , quantifying ecohydrological interactions and the origin of atmospheric moisture (i.e. evaporation or condensation; Gao et al.,). Recent developments in using *in-situ* measurements of stable water isotopes are making use of non-destructive online monitoring techniques and are increasingly advanced . In terms of analyzing δ_v , grab samples or refrigerated traps for offline analysis in the laboratory were already used in the 1990s with rapidly accelerating progress in recent years . Today, CRDS techniques have been shown to be useful for measuring δ_v at continuously high-resolution and thus, enabling real-time analysis of δ_v which can give more novel insights than precipitation alone . For example, the technique has been successfully deployed for monitoring sub-tropical sub-cloud raindrop evaporation ; for testing vapour equilibrium assumption for $\delta^{18}\text{O}$ cellulose estimates ; diurnal and intra-seasonal variations in evaporative signals at different heights above the Greenland ice sheet ; and to characterise variation in δ_v and their controlling factors during extreme precipitation events . To date, however, hardly any *in-situ* studies have assessed δ_v dynamics in the urban atmospheric boundary.

Previous isotopic studies have reported contrasting ecohydrological partitioning under different land use types in urban green spaces . A study in Scotland assessed land use influences on isotopic variability revealing that urbanisation, intensive agriculture and responsive soils caused rapid cycling of precipitation to stream water . Others found higher ET and older groundwater recharge beneath urban trees, but more marked soil evaporative losses under grassland . By integrating simple modelling and observational water isotope data, Stevenson et al. quantified the heterogeneities in urban ecohydrological partitioning and found that median ET increased from grassland, to evergreen shrub, to larger deciduous forest through to larger conifer trees, with groundwater recharge behaving contrary. Mixing models applied to different Berlin green spaces showed that trees were more dependent on deeper, older sub-soil and groundwater sources, whereas grass very probably recycled shallow, younger soil water in transpiration . Such isotopic information of water fluxes through the critical zone can be used in ecohydrological models that can resolve ET into its component parts. However, to do this, the isotopic gradient at the atmospheric-land interface is usually defined in models assuming δ_v is in equilibrium with current or recent rainfall . Despite now being logistically possible, monitoring δ_v *in-situ* at different heights and above vegetation canopies is still rare. Braden-Behrens et al. demonstrated the value of direct *in-situ* eddy covariance measurements of δ_v in the surface boundary layer. Despite standard model assumptions of an equilibrium between δ_v and precipitation, δ_v can be out of equilibrium with local water sources and can show gradual depletion with altitude . High-resolution *in-situ* monitoring of δ_v allows testing of such equilibrium assumptions, but so far, very few studies have tested this with *in-situ* ambient data .

Here, we conducted a “proof of concept” study to assess the changing isotopic composition of δ_v over a 2.5 months period in an urban green space with contrasting landcover. We deployed a laser spectrometer in the field for continuous *in-situ* monitoring of δ_v in the urban surface boundary layer. Our overarching research question was whether we can generate data with *in-situ* real-time sequential monitoring that increases our understanding of origins of atmospheric moisture and its link to water partitioning by contrasting urban vegetation. Our specific objectives were to:

1. investigate dynamics in δ_v within two contrasting urban vegetation types to understand what types of landcover enhance moisture fluxes back to the atmosphere.
2. investigate these changes in relation to related ecohydrological dynamics of soil moisture storage, sap flow rates and biomass accumulation.
3. assess the extent of equilibrium between vapour and precipitation.

Based on these assessments, we discuss the future value, challenges and potential in gaining and processing such high-resolution data to improve understanding of ET partitioning at different heights in the atmosphere above different types of landcover in urban green spaces, which would be important for increased process understanding across urban critical zones.

2. Study Site

The experiment was carried out in the SE of Berlin, Germany (Fig. 1). Berlin is located on the flat North European Plain where the topography and geology are dominated by deposits from the Pleistocene glaciation. The climate is continental temperate with long-term (1981–2010) mean annual rainfall of 577–602 mm ranging between stations and mean annual air temperatures of 9.4–10.2 °C. Berlin covers 891 km², with a population of 3.66 million (, 2020; Fig. 1B). The majority of the city is covered by residential areas and streets (~59%), but there are large amounts of green and blue spaces: vegetation covers ~34% (forests, parks, agriculture) plus ~7% surface waters.

Our study site is located at the grounds of the Leibniz-Institute of Freshwater Ecology and Inland Fisheries (IGB), roughly 220 m north of Lake Müggelsee (Berlin’s largest lake) (Fig. 1B). The geology is characterized by sand and gravel deposits of the Berlin-Warsaw glacial spillway, (, SenUVK online, 2007). The surrounding district (Fig. 1B) is characterized by residential areas and roads (38 %), forest (40 %), water bodies (12 %) and public green space (0.06 %;). The study site is a park-like space with older trees (~30–100 years old) surrounded by brick buildings of former 19th century water works and extensive rough grassland above subsurface slow sand filter systems, which were used for drinking water treatment until the beginning of the 1990s (, online). Within a 100 m radius of the study site center (Fig 1C), premises are covered by buildings (10 %), different types of non-irrigated urban green spaces, including grassland (49 %), shrubs (8 %) and trees (17 %); and streets, semi-permeable or sealed pathways and parking spaces (16 %).

The experiment focused on two small areas; one tree dominated, the other grassland dominated and 16 m apart (Fig 1C). The grassland site was covered by grass (e.g. *Lolium perenne*, *Arrhenatherum elatius*) and herbs (e.g. *Trifolium pratense*, *Achillea millefolium*) of 30–50 cm height, mowed twice a year and can be referred to as an urban meadow. The tree site was dominated by black locust, lime, oak, birch and maple trees. We selected one dominant maple tree (*Acer platanoides*) with a stem diameter of 550 mm (August 2021) and height of ~16 m. In other studies, *Acer platanoides* has been shown to have a high drought tolerance and can maintain low leaf gas exchange rates.

The soils reflect anthropogenic impacts, such as partly backfilled ground after construction work. They are classified as Anthrosols (SenUVK, , 2017, online), which consist of debris, sandy materials and a shallow humus layer from extensive gardening.

3. Data and Methods

3.1. Monitoring

The study period was from August 20th to November 3rd 2021. Climate data (air temperature, precipitation amount, wind speed and direction, relative humidity, air pressure, global radiation) were available from the rooftop of IGB ~300 m away. Additionally on site, precipitation (tipping bucket raingauge, 0.2 mm/tip, precision ±3% of total rainfall; AeroCone® Rain Collector, Davis Instruments, Hayward, USA) was recorded with a CR800 Datalogger (Campbell Scientific, Inc. Logan, USA) logging every 15 min. Temperature was recorded (every 5 min) with BetaTherm 100K6A1IA Thermistors T107 (Campbell Scientific, Inc. Logan, USA; tolerance ±0.2°C (over 0°–50°C)), with a CR300 Datalogger (Campbell Scientific, Inc. Logan, USA). Precipitation and temperature data were verified against available data from the German Weather Service (DWD) of the “Berlin-Marzahn” station (Station ID: 420), ~12 km north of the study site.

Precipitation for stable water isotope analysis was collected using a HDPE deposition sampler (100 cm² opening; Umwelt-Geräte-Technik GmbH, Müncheberg, Germany). Overall, 32 daily and 15 bulk (interval ~weekly) samples with precipitation >1 mm (to limit evaporation effects) were collected between July and November 2021. Further, daily precipitation samples were collected ~350 m away from the study site with an autosampler (ISCO 3700, Teledyne Isco, Lincoln, USA) at a 24 hours interval. All autosampler bottles were filled with a paraffin oil layer > 0.5 cm in thickness (after IAEA/GNIP, 2014) to avoid evaporative

effects. Additionally, groundwater samples were taken weekly with a submersible pump (COMET-Pumpen Systemtechnik GmbH & Co. KG, Pfaffschwende, Germany) from a well on IGB grounds ~300 m away from the site.

For isotope analysis of the liquid water samples at the IGB laboratory, samples were filtered (0.2 µm cellulose acetate) and decanted into 1.5 ml glass vials (LLG LABWARE). They were analysed by cavity ring-down spectroscopy (CRDS) with a L2130-i Isotopic Water Analyser (PICARRO, INC., Santa Clara, CA) using four standards for a linear correction function and which were referenced against three primary standards of the International Atomic Energy Agency (IAEA) for calibration (VSMOW2 (Vienna Standard Mean Ocean Water 2), GRESP (Greenland Summit Precipitation) and SLAP2 (Standard Light Antarctic Precipitation 2)). Liquid samples were injected six times and the first three injections discarded. To screen for interference from organics, the ChemCorrect software (Picarro, Inc.) was applied and contaminated samples discarded. After quality-checking and averaging multiple analyses for each sample, the results were expressed in δ -notation with Vienna Standard Mean Ocean Water (VSMOW). Analytical precision was 0.05 for $\delta^{18}\text{O}$ and 0.14

Stable isotopes of atmospheric water vapour (δ_v) were measured *in-situ* at the tree-dominated and grassland sites, respectively at 0.15 m, 2 m and 10 m height to capture the effects of vegetation heterogeneity and potential turbulence within an urban surface boundary layer. To monitor the elevation profile above the grassland, a 10 m flag mast with ~ 100 cm long perpendicular poles at required sample points was set up (Fig. 2). At the tree site, we measured directly at the trunk within the canopy of the maple tree. The measurement campaign started on 20.08.2021 above the grassland and on 03.09.2021 in the tree canopy.

We performed *in-situ* real-time sequential measurements of water vapour via CRDS (Picarro L2130-i, Picarro Inc., Santa Clara, CA, USA) placed in a box between the sampling sites. Air inlets and CRDS were connected with polytetrafluoroethylene (PTFE) tubing (1.6 mm x 3.2 mm). We used PET bottles covered with aluminum foil to prevent the inlets from rain and sun exposure. Each tube inlet (Fig. 2) was sampled for 20 min in resolution of seconds. Then sampling was switched automatically to the next one; resulting in a 2-hourly resolution for each inlet. We only used the data when a measurement showed stable values (i.e. ranges of 2). The first 5 min of data after switching inlets were always discarded to avoid memory effects. Prior the vapour entering the CRDS unit, a preceding sub-micron particulate filter was connected to prevent liquid water from entering by creating a low dew point by lowering the air pressure. The sample flow rate was at 0.04 L min^{-1} . Water vapour concentrations were always above 6000 ppm (this is where the concentration dependent deviation becomes low and thus measurement precision is not compromised).

To allow for later conversion of δ_v measurements into liquid water isotope values, temperature probes were installed at all heights near the tube inlets at both sites with BetaTherm 100K6A1IA Thermistors T107 (Campbell Scientific, Inc. Logan, USA; tolerance $\pm 0.2^\circ\text{C}$ (over $0^\circ\text{--}50^\circ\text{C}$)), with a CR300 Datalogger (Campbell Scientific, Inc. Logan, USA) logging mean values every 5 min from secondly-resolved data. To avoid tube condensation, heating cables (ILLw.CT/Qx, Quintex GmbH, Lauda-Königshofen, Germany) were installed and wrapped with the tube in insulation material. The cables were controlled via an automatic multi socket (Gembird 235 EG-PMS2, Gembird Software Ltd., Almere, The Netherlands) to prevent overheating in summer. To minimise condensation effects, the measurements were checked daily. The PTFE-tubes were flushed weekly or if required for 10 minutes per probe to remove any water. Data was discarded when condensation inside the system was identified in the respective tube.

By combining δ_v and temperature data from each inlet we derived the values for all heights of temperature dependent equilibrium fractionation from vapour to liquid with the correction formulated by Majoube :

$$\alpha = \exp\left(\frac{a\left(\frac{10^6}{T_k^2}\right) + b\left(\frac{10^3}{T_k}\right) + c}{1000}\right) \quad (1)$$

where a is the isotopic fractionation factor, T_k is the temperature (in K), and a , b , and c are empirical parameters that vary depending on the isotopologue. All values of isotopic compositions are given in liquid

phase and relative to Vienna Standard Mean Ocean Water (VSMOW).

To investigate the local evaporative effects, the line-conditioned excess (short lc-excess) (see) was calculated. The lc-excess describes the deviation of the sample from the local meteoric water line (LMWL):

$$\text{lc-excess} = \delta^2\text{H} - a \cdot \delta^{18}\text{O} - b \quad (2)$$

where a is the slope and b the intercept of the weighted isotopic composition of the local precipitation. The LMWL was calculated by amount-weighted least square regression from daily precipitation isotopes measured at IGB from July until November 2021.

In order to assure stable values to offset variability in the field, stability of the CRDS was tested in the lab before installing the setup outside. During the sampling campaign, we calibrated once a week (cf. calibration periods) with two standards. Stored in sealed glass containers, the standards were connected to the CRDS for two-point calibrations (liquid values: light: ^2H -109.91 concentrations and added linear regressions of temperature dependency slopes to correct for isotopic offsets and vapour concentration dependency (resembling the approach by Schmidt et al.).

We also monitored sap velocities and stem circumference of the maple tree. Two sap flow sensors (SFM-4, Umwelt-Geräte-Technik GmbH, Müncheberg, Germany; ± 0.1 cm/hr heat velocity precision) were installed at breast height (1.3 m) at the north and south side of the tree stem. The sap flow sensors work according to the heat ratio method by Marshall . Daily reference crop evapotranspiration (ET_0) was estimated using the FAO Penman–Monteith method with “R”-Package “Evapotranspiration” . To investigate dynamics during the growing season, both daily mean sap velocity [cm h^{-1}] and ET_0 were then normalized (to $\text{sapvelocity}_{\text{norm}}$ and ET_{norm} , respectively) by feature scaling. One dendrometer (DR Radius Dendrometer, Ecomatik, Dachau, Ger170; accuracy max. $\pm 4.5\%$ of the measured value (stable offset)) was also installed to measure stem diameter dynamics at high temporal resolution. Sap velocity and stem increments were logged as 15 min intervals using a CR300 Datalogger (Campbell Scientific, Inc. Logan, USA). Throughfall amount was sampled manually at a height of 30 cm above ground using four rain gauges (Rain gauge kit, S. Brannan & Sons, Cleator Moor, UK) which were installed 1 m and 3 m, respectively, north and south of the tree’s stem.

Volumetric soil water content and soil temperature were measured at both sites (Fig. 2) by soil moisture temperature probes (SMT-100, Umwelt-Geräte-Technik GmbH, Müncheberg, Germany) in the upper soil at 6 cm depth. Recording took place with a CR800 Datalogger (Campbell Scientific, Inc. Logan, USA) with a 15 min frequency and a precision of $\pm 3\%$ for volumetric soil water content and ± 0.2 °C for soil temperature. Groundwater level in one well was monitored with an automatic datalogger (groundwater level probe) at an interval of 15 min (see location in Fig. 1C).

3.2 Testing differences, correlations and the equilibrium assumption

In order to analyse differences and correlations of the data, we performed several statistical tests. Each dataset was tested for normality using Shapiro-Wilk . If normally distributed, we performed simple t -statistics to test for significant differences. If data were skewed or non-normal, we performed non-parametric alternatives: Wilcoxon signed-rank test for two groups and Kruskal-Wallis test by ranks for more than two groups . To test correlations of non-linear data we applied Spearman’s rho statistic .

Due to the nature of the high-resolution dataset of δ_v , we could also test the equilibrium assumption of δ_v and precipitation for the sampling period using the following equation:

$$R_{\text{atm}} = R_v - R_p \quad (3)$$

where R_v and R_p are the liquid Majoube-corrected isotope ratios of δ_v and liquid isotope ratios of precipitation and $\Delta P_{\alpha\tau\mu}$ is the difference in isotope ratios of water vapour and precipitation in atmosphere. These laboratory standards are also relative to VSMOW. If $\Delta P_{\alpha\tau\mu} = 0$, a perfect equilibrium between precipitation and δ_v isotope ratios prevails. We used the daily mean of δ_v at 2 m height for the tree site and grassland site separately to compare both types of landcover. $\Delta P_{\alpha\tau\mu}$ was calculated for days when precipitation occurred.

4. Results

Hydroclimate

Figure 3 shows the variability in hydroclimatic variables during the study period in the context of a longer 6-month period. Summer and autumn precipitation were close to the seasonal average; with a large convective event in July and numerous smaller events in August and September when monitoring was ongoing. Air temperatures reflected radiation, and decreased from July until December, though they were also near-average in the monitoring period. Relative humidity was lower in summer, when temperatures were highest and declined thereafter. Wind speeds were low (<1 m/s) through most of the sampling.

4.2 Ecohydrological dynamics

Throughfall (> 1 mm; not shown) only occurred during three major precipitation events and varied between the sampling points underneath the canopy as follows: 2.8 - 5.5 mm on 15.09., 9-15 mm on 29.09 and 2.5-4.8 mm on 24.10. Soil moisture in the upper soils rapidly responded to rainfall at both sites, though quickly dried until more persistent rewetting towards November (Fig 4b). The tree site soil was generally more responsive to wetting particularly following heavy rainfall on September 29th. The average groundwater level (Fig 4b) was around 2.3 m b.g.l. and varied only by 2cm as it was primarily controlled by the water levels in the lake.

Daily mean sap velocity ranged from 0-9.2 cm h^{-1} (0-0.92 m h^{-1} ; Fig. 4c-d). The southern side of the tree showed higher values but similar dynamics until October. Towards the end of the growing period, the northern side had slightly higher sap velocities. Cumulative increments of stem size showed progressive growth between the end of August and November. Normalised for mean sap velocity, $\text{sapvelocity}_{\text{norm}}$ showed the same ranges as mean ET_{norm} (i.e. also normalized against the mean) from August until mid-October, implying there was no limit on the trees meeting atmospheric moisture demand. As leaf senescence and fall progresses in the middle of October, ET_{norm} exceeded $\text{sapvelocity}_{\text{norm}}$.

Stable water isotope dynamics

Figure 5 shows that stable water isotopes in precipitation were highly variable and showing more negative values (i.e. high depletion in heavier isotopes) for events in late August and early November. δ_v at the tree and grassland sites (both exemplary shown for 2 m height) was influenced by depleted rainfall inputs. For example, δ_v at the grassland sites (prior to tree monitoring commencing) showed particularly high depletion in response to depleted rainfall at the beginning of September (Fig 5a). Summary statistics of measured stable water isotope values and ranges of precipitation, groundwater and atmospheric vapour δv (liquid values) are given in Table 1.

After testing Spearman's rank correlation between δ_v and soil moisture at both sites for different heights, only the grassland site indicated a significant positive correlation of soil moisture with $\delta^2\text{H}$ of δ_v (0.3 at 0.15 m; 0.24 at 2 m; 0.22 at 10 m), but none for $\delta^{18}\text{O}$. The tree site showed no significant correlations between δ_v and soil moisture for either isotope.

Lc-excess in precipitation increased from late summer to late autumn, though variability remained high especially in October. The lc-excess was generally negative at both sites until mid-September (Fig. 5b), reflecting high energy for evaporation. From Mid-September until November, lc-excess of δ_v was generally positive but more variable. Spearman rank correlation coefficients between precipitation and δ_v were 0.55 for $\delta^2\text{H}$ and 0.43 for lc-excess indicating positive correlations.

The amount-weighted LMWL of the sampling period (July – November 2021) (Fig. 6) was $\delta^2\text{H} = 7.71 \pm 0.11 * \delta^{18}\text{O} + 7.42 \pm 1.12$ ($R^2 = 0.987$). The dual isotope plot (Fig 6) clearly shows that precipitation isotopes were characterized by large ranges ($\delta^2\text{H}$ -145.2 showed little variation with mean isotopic signatures (Tab. 1). Beneath the tree canopy, δ_v was more homogenous across the elevation profile than above grass. Grassland showed a higher variance of ambient vapour within the elevation profile, with a tendency of near-surface air (0.15 m height) to be more enriched in heavier isotopes in comparison to the tree-site surface air, but

attenuating with height (Tab. 1). Overall, the boxplots and median values of grassland δ_v showed a slightly higher range compared to the tree site (Fig 6, Tab 1). The Kruskal-Wallis-Test showed significant differences of δ_v (p-values < 0.05) between ground-level (0.15 m) and higher elevations (2 m, 10 m) at the grassland, while there were no significant differences (p-values > 0.05) between different heights underneath the tree canopy and also no significant differences between both sites. The Wilcoxon signed-rank test indicated a p-value of 0.0507 ($\alpha=0.05$) between the sites for 0.15 m height showing they were significantly different.

We also investigated higher resolution dynamics of δ_v during precipitation events, and we display here the event on the afternoon of 15.09.2021 (where 6.6 mm fell between 15:00 – 18:30; Fig. 7). Both sites showed enriched δ_v values at night corresponding to the signature of precipitation, with uniform distribution at different heights. The next day, δ_v above grassland reflected clear evaporative losses by more enriched values just above the surface, where windspeed and soil moisture was higher, which was also observed during the other events. In the tree canopy, no differences with height occurred. During the event, soil water content underneath the tree was 4.2 % and increased to 5.6 % 24 h after the rainfall; whereas the grassland was wetter increasing from 5.0 % to 8.7 % (see also Fig. 4). A common aspect for all the precipitation events was a close link between precipitation isotopic signature and δ_v .

4.4 Equilibrium between vapour and precipitation

The difference in isotope ratios of δ_v and precipitation in the atmosphere, $\Delta P_{\alpha\tau\mu}$, generally differed from zero (i.e. the equilibrium) at both sites, with higher deviation from the equilibrium between mid-August and mid-September (Fig. 8). Responses of $\Delta P_{\alpha\tau\mu}$ after precipitation events showed heterogenous patterns, reflecting varying differences from the equilibrium throughout the monitoring period. In August, grassland showed only positive $\Delta P_{\alpha\tau\mu}$, depicting more enriched δ_v compared to precipitation. On an event basis, grassland and tree sites differed slightly in $\Delta P_{\alpha\tau\mu}$ and the timeseries of $\Delta P_{\alpha\tau\mu}$ for $\delta^{18}\text{O}$ and $\delta^2\text{H}$ showed similar patterns.

Boxplots showed higher $\Delta P_{\alpha\tau\mu}$ values at the grassland site (though note that grassland included more data, Fig. 9). T-tests did not show significant differences between grassland and tree site for $\Delta P_{\alpha\tau\mu}$ $\delta^2\text{H}$ (p=0.055) but showed significance for $\Delta P_{\alpha\tau\mu}$ $\delta^{18}\text{O}$ (p=0.012), again showing a difference between the two vegetation types in their variation from equilibrium. Median $\Delta P_{\alpha\tau\mu}$ values of $\delta^2\text{H}$ were 2.95 at the grassland, and 0.51 $\delta^{18}\text{O}$ at the tree site. Maximum and minimum $\Delta P_{\alpha\tau\mu}$ values at the grassland ranged between -30 and 46 $\delta^{18}\text{O}$, respectively. At the tree site they varied between -31 and 26 $\delta^{18}\text{O}$, respectively. Thus, the difference from equilibrium of δ_v with precipitation was greater at the grassland than at the tree stand. The higher and more abundant positive values at grassland reflect a higher isotopic enrichment of δ_v .

5. Discussion

5.1 Vapour stable water isotopes in different urban vegetation

This study showed that extended (i.e. >2 months) periods, continuous sequential *in-situ* monitoring of δ_v produces reliable ad novel data in urban green space environments with a temperate climate. Our distributed network of inlet ports sampling the atmospheric boundary at different heights above contrasting urban green space vegetation produced reliable high-resolution data with a 2-hourly resolution for each inlet. However, there is no doubt that the method is very labour intensive and requires almost daily maintenance including checking the correct operation of the CRDS, ventilation systems and pumps. Detailed, biweekly data checks of the different inlets are also necessary to detect condensation in the tubes or other unwanted memory effects in the CRDS. In particular, the *in-situ* setup requires a secured environment for the CRDS and vapour tubing (e.g. a locked and fenced box and securing pipes adapted to the study site). Overall, however, *in-situ* monitoring of δ_v needs less regular maintenance than *in-situ* soil water monitoring due to greater condensation issues from deep soil compared to atmospheric vapour (cf.).

Monitored δ_v data fluctuated around the LMWL in equal distribution over the entire study period indicating no dominance of non-equilibrium fractionation, but disequilibrium occurred at shorter time scales. We found limited difference between the two vegetation covers reflecting a generally well mixed boundary. δ_v of grassland showed a slightly higher temporal variability and also higher variance along the height profile compared to the tree site. The only significant difference was that the surface air (at 0.15 m height) above the grassland was more enriched, though this was rapidly attenuated with height. An *in-situ* study by Griffis et al. found similar effects of surface evaporation enriching surface boundary layer water vapour and atmospheric loss of light vapour fraction above grassland through the underlying process of kinetic fractionation during evaporation, while tree canopy protects from such loss.

At the event scale, δ_v showed clear isotopic responses after rain. The response timing was dependent on the time of day being more marked around noon when radiation input is elevated. This is due to the fact that δ_v at hourly timescale is controlled by air mass advection which increases with higher solar radiation. At seasonal scale, lc-excess was low in summer and higher in autumn reflecting higher ET in warmer months. Griffis et al. explained the seasonal amplitude of δ_v to be driven by Rayleigh processes that are strongly modulated by evaporation and entrainment, i.e. inflow of an air parcel to another.

5.2 Insights into high-resolution urban ecohydrology

Our results indicate that the urban grassland surface is contributing to the atmospheric moisture affecting water partitioning with the main drivers being high surface evaporation and/or high transpiration of the grass, high surface temperatures as well as low atmospheric mixing. The measurements from beneath canopy give useful insights for turbulent mixing parameterisation of urban canopy layer vertical transport, but direct transpiration imprint could not be measured.

Additional insights into the processes controlling isotopic composition of urban green space δ_v were leveraged by having simultaneous ecohydrological monitoring, i.e. measurements of soil moisture, throughfall, sap flux and tree diameter. At both sites, the overall low top soil moisture increased in response to precipitation and then decreased with time reflecting drainage and evaporative losses that contribute – at least in the grass plot – to increased evaporation that affects the isotopic signal at 0.15 m. Potential normalized ET_{norm} did not exceed total sap flux_{norm} of the maple tree during the phase of active leaves indicating no drought stress of the tree. Additionally, dendrometer data revealed normal stem growth for late summer and autumn. Considering the low top soil moisture and constant sap flux, our results match with the findings of Kuhlemann et al., from another urban green space site in Berlin in that urban tree transpiration rates show a certain resilience to drought (which is of course highly dependent on tree ages and species). Further, the investigated tree stands were a group of trees which probably makes a difference compared to individual urban trees in another study that showed considerably higher sap flux densities.

Interestingly, despite interception evaporation and transpiration from the urban tree canopy after events, there was no imprint on δ_v captured at 10 m compared to lower heights (cf. δ_v variabilities did not correlate with certain ecohydrological parameters throughout the whole sampling period; though δ_v responded to changes in potential ET during the warmer period until the end of September. A storm on Oct. 21st led to a quick decrease of δ_v signatures that day.

These insights on high-resolution dynamics of ecohydrological fluxes and partitioning can contribute to improved strategies of urban green space management in the future. However, there is great potential for more detailed monitoring of urban canopy ET by more distributed networks in canopies, e.g. it would be interesting to measure at least 5 m over an urban canopy or higher similar to Braden-Behrens et al. and compare this with corresponding measurements above an urban grassland.

5.3 Testing the assumption of equilibrium between vapour and precipitation

The equilibrium assumption between the isotopic signatures of δ_v and precipitation was not always held during our field campaign. Previous studies showed that the equilibrium assumption is more robust at subseasonal, longer time scales than for individual rain events. Lee et al. found that during rain events, vapour in the surface layer developed in general a state of equilibrium with the falling raindrops. In our study, this assumption was not robust at the subseasonal scale and did not confirm an establishment of an equilibrium.

ΔP_{atm} (i.e. difference in isotope ratios of water vapour and precipitation in atmosphere) was greater and showed more positive values in summer reflecting that vapour was more enriched than precipitation during summer. Potential reasons for these results are (as discussed by): raindrops formed at high elevation , precipitation came from convective events with big raindrops or high tree transpiration rates from deeper sources prevented vapour from equilibrium with precipitation. Additionally, high transpiration rates lead to isotopic enrichment of δ_v and could generate higher deviation from δ_v with precipitation.

Testing the equilibrium assumption is especially important for areas with a distinct microclimate like cities as previous studies showed that equilibrium estimates can be biased . Further, different regions of the World show diverging results for ΔP_{atm} depending on climate, altitude and latitude. E.g. Mercer et al. showed that the equilibrium assumption does not hold in continental mountain environments. By going beyond the standard assumption of equilibrium in urban ecohydrology, we can improve simple mixing models, complex process-based, isotope-aided ecohydrological models like Ech₂O-iso , estimations in keeling plot and the Craig and Gordon approach (cf.).

6. Conclusion

We monitored stable water isotopes in liquid precipitation and atmospheric water vapour (δ_v) using *in-situ* cavity ring-down spectroscopy (CRDS) over a two-month period in an urban green space area in Berlin, Germany. δ_v was monitored at multiple heights (0.15, 2 and 10 m) in different vegetation: grassland and forest plots. Our distributed sampling network of inlet ports produced novel, reliable high-resolution data with a 2-hourly resolution for each inlet.

We have shown that the isotopic composition of δ_v above both land uses was highly dynamic and positively correlated with that of rainfall indicating the changing sources of atmospheric moisture. The isotopic composition of δ_v was similar across most heights of the 10 m profiles and between the two plots indicating limited aerodynamic mixing. Only the surface at ~ 0.15 m height above the grassland showed significant differences in δ_v , with more enriched values indicative of evaporative fractionation immediately after rainfall events.

We combined this isotope monitoring with hydroclimatic monitoring and measurements of sap flow, stem size, soil moisture, throughfall. At both sites, the overall low top soil moisture increased in response to precipitation and then decreased after the events reflecting drainage and evaporative losses. Potential normalized ET_{norm} did not exceed total sap flux_{norm} of the maple tree during the phase of active leaves indicating no drought stress on the tree. Dendrometer data revealed normal stem growth for late summer and autumn. Despite interception evaporation and transpiration from the tree canopy after events, there was no imprint on δ_v captured at 10 m compared to lower heights. Our results indicate occasional dis-equilibrium between water vapour and precipitation isotopes.

Our set up provided novel insights into high-resolution dynamics of water cycling and partitioning in across the Critical Zone of an urban green space can contribute to improved urban planning strategies providing new evidence-base. Such data has the potential to better constrain the isotopic interface between the atmosphere

and the land surface. Importantly, it can be incorporated into tracer-aided ecohydrological models that can resolve evapotranspiration fluxes and improve these estimations.

However, more research is needed to upscale these findings to canopy and city scale. More detailed monitoring of urban canopy ET by more distributed networks in and above canopies will benefit further investigations.

Acknowledgements

This study was funded through the German Research Foundation (DFG) as part of the Research Training Group “Urban Water Interfaces” (UWI; GRK2032/2) and the Einstein Foundation as part of the “Modelling surface and groundwater with isotopes in urban catchments” (MOSAIC) project. Funding for DT was also received through the Einstein Research Unit “Climate and Water under Change” from the Einstein Foundation Berlin and Berlin University Alliance (grant no. ERU-2020-609) and the project BiNatur (BMBF No. 16LW0156). We also acknowledge the BMBF (funding code 033W034A), which supported the stable isotope laboratory and in-situ laser analyser. Contributions from CS have also been supported by the Leverhulme Trust through the ISO-LAND project (grant no. RPG 2018 375). We thank all colleagues involved in the ecohydrological monitoring and daily precipitation and groundwater sampling, but in particular are grateful to Jan Christopher, Jonas Freymüller and Jessica Landgraf.

Figures

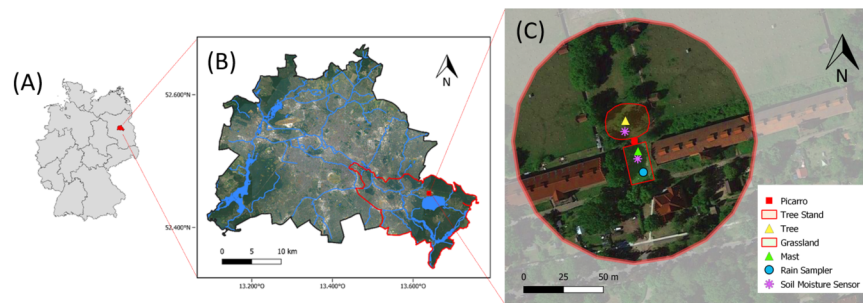


Fig. 1. Location of Berlin within Germany and map of Berlin (A, B); and the study site at IGB Berlin (C) with the two sampling sites (75 m radius from center) grassland with flagmast and tree site with *Acer platanoides*; and installations of atmospheric water vapour in-situ measurements, sap flow and soil moisture measurements and precipitation sampler. (Basemap: Google Satellite)

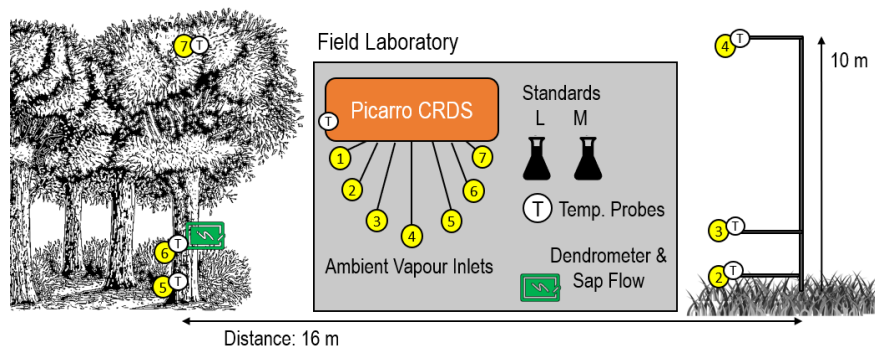


Figure 2. Conceptual diagram of the general in-situ isotope measuring setup. Numbers refer to different tube inlets for vapour (1 refers to a reference inlet at the CRDS).

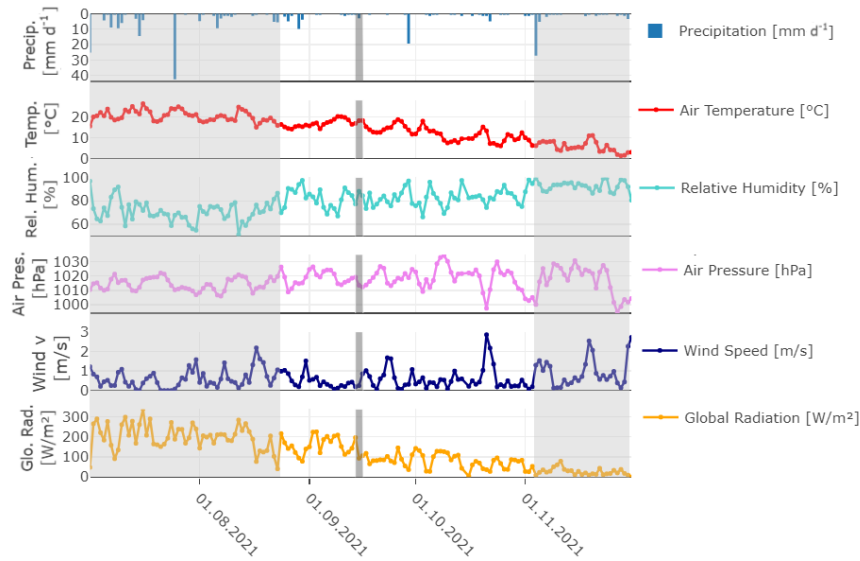


Figure 3. Time series of daily climate data during the study period (July – November 2021) (precipitation [mm], air temperature [°C], relative humidity [%], windspeed [m/s], global radiation [W/m²]) with periods before and after CRDS measurements shaded in grey and the in detail investigated event marked with a grey bar (see Figure 7).

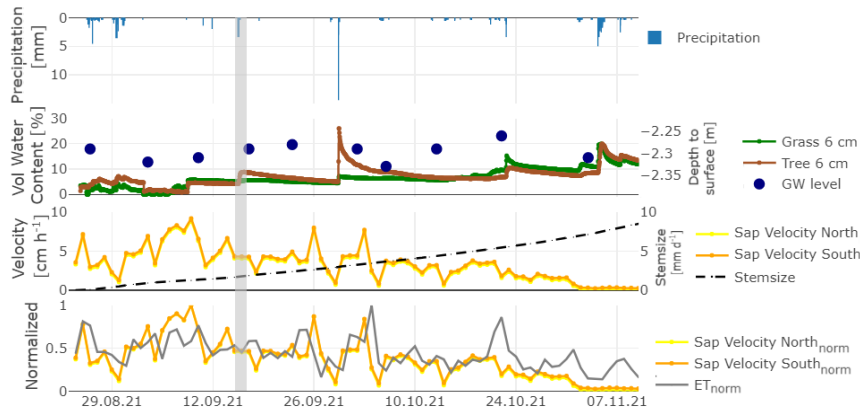


Figure 4. a) Precipitation [mm] (focus precipitation event marked). b) Soil moisture (VWC [%*h⁻¹]) and groundwater levels (measured every 2 weeks). c) Daily mean sap velocities measured at the maple tree and daily stem size variation as cumulative increments (measured for the stem-radius). d) Daily normalized sap velocity ($sapvelocity_{norm}$) and normalized Evapotranspiration (ET_{norm}).

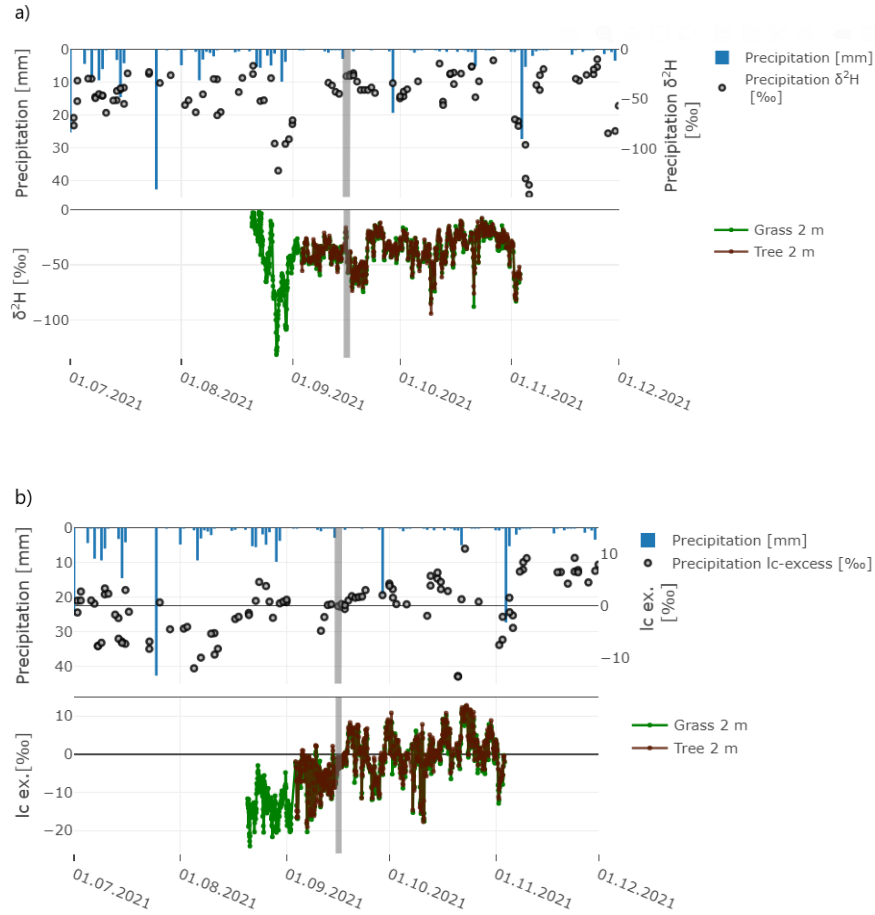


Figure 5. Precipitation amount, daily stable water isotope ratios of precipitation and hourly δ_v of the tree site and grassland (both at 2 m height) for (a) ^2H of δ_v and (b) lc-excess of δ_v (focus precipitation event marked).

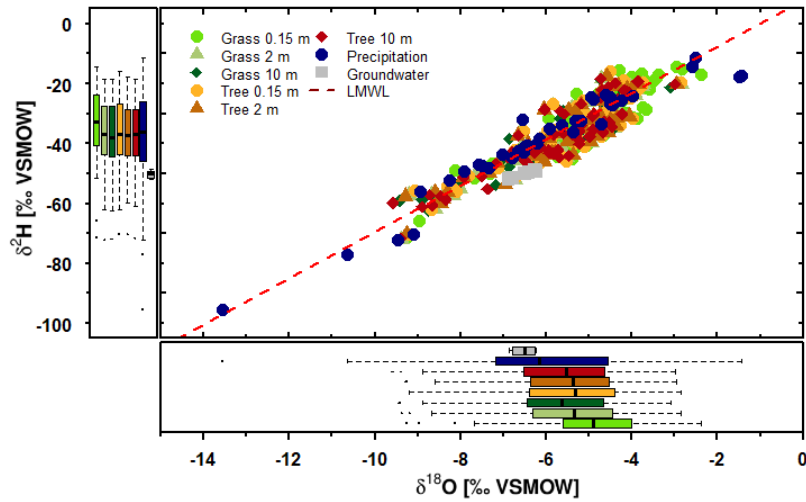


Figure 6. Dual isotope plot of δ_v

(shown as daily mean) of the different heights and vegetation types as well as precipitation (daily) and groundwater (weekly). Data shown here were sampled between 04.09. and 03.11.2021, when sampling was active on both sites. Boxplots show the sample distribution of the data sets.

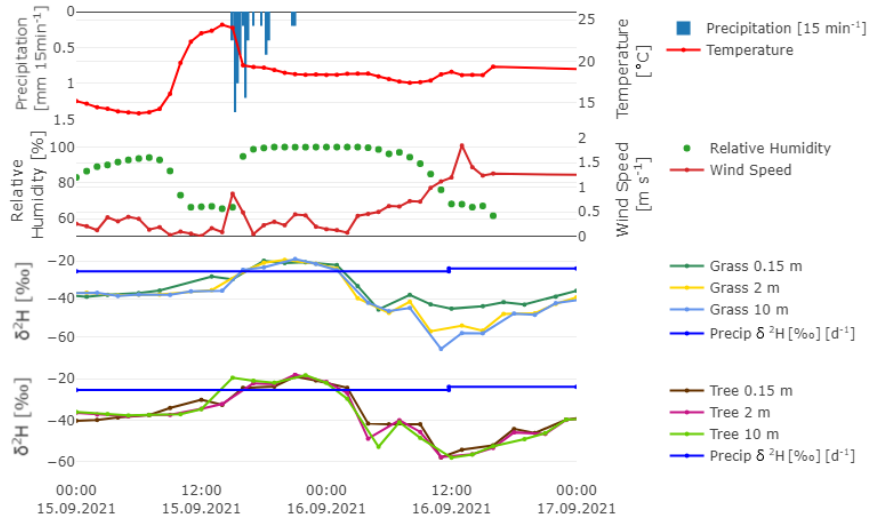


Figure 7. Responses of 2H_v to the precipitation event on 15.09.2021 at the two sites.

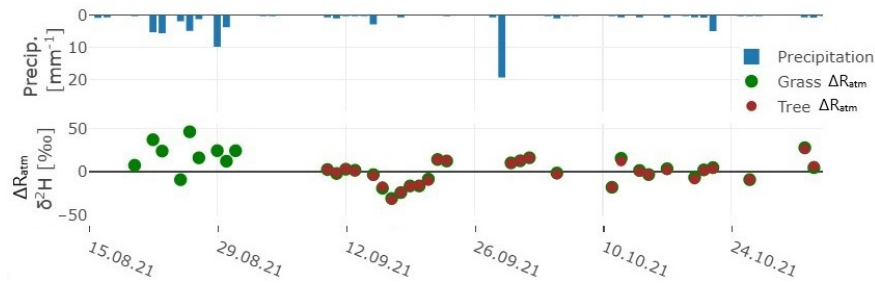


Figure 8. $\Delta R_{atm} \delta^2H$ οφ $\delta^{18}O$ ανδ δ^2H at 2 μ ηγειητ φορ γρασλανδ (γρεεν) ανδ τρεε σιτε (βρωων) βασειδ ον οσσυρρινγ πρεσιπιτατιον εεντς (δαιλιφ αμιουντς).

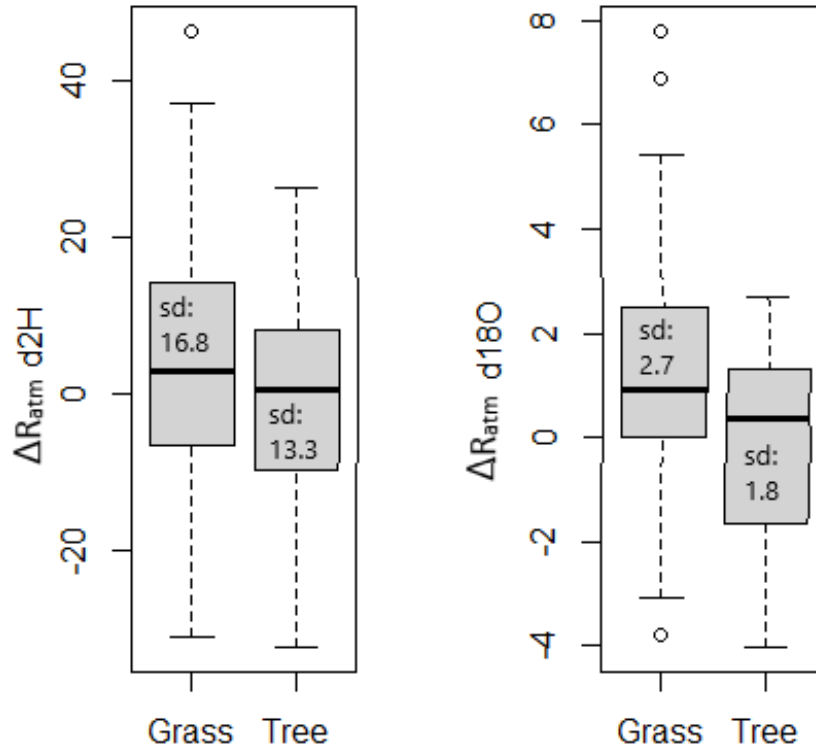


Figure 9. ΔP_{atm} διστριβυτιονς οφ $\delta^{18}\text{O}$ ανδ $\delta^2\text{H}$ οφ τηε γρασσανδ ανδ τρεε σιτε ατ 2 μ ηειγητ δυρινγ τηε σαμπλων περιοδ.

Tables

Table 1. Summary statistics of measured stable water isotope values of precipitation, groundwater and atmospheric vapour δ_v (liquid values).

	%o	min	mean	max	median	sd
Precipitation	$\delta^2\text{H}$	-145.22	-46.13	-10.161	-40.8	26.27
	$\delta^{18}\text{O}$	-19.25	-6.94	-1.44	-6.2	3.39
	lc-excess	-13.6	-0.06	10.93	0.67	5.16
Groundwater	$\delta^2\text{H}$	-55.83	-51.17	-47.99	-49.8	2.91
	$\delta^{18}\text{O}$	-7.63	-6.68	-5.94	-6.44	0.59
	lc-excess	-9.58	-7.05	-4.41	-7.6	1.66
Vapour						
Grass 0.15 m	$\delta^2\text{H}$	-163.91	-116.39	-87.17	-32.53	12.75
	$\delta^{18}\text{O}$	-21.01	-15.35	-11.43	-4.81	1.68
	lc-excess	-23.36	-5.49	8.38	-5.07	5.87
Grass 2 m	$\delta^2\text{H}$	-165.96	-119.82	-94.9	-35.6	13.23
	$\delta^{18}\text{O}$	-22.3	-15.88	-12.06	-5.22	1.85
	lc-excess	-25.16	-4.84	7.32	-4.53	5.92
Grass 10 m	$\delta^2\text{H}$	-169.92	-120.52	-85.61	-36.13	13.73
	$\delta^{18}\text{O}$	-22.59	-16.05	-12.1	-5.38	1.88
	lc-excess	-20.93	-4.19	8.58	-4.11	5.33
Tree 0.15 m	$\delta^2\text{H}$	-164.3	-119.43	-92.33	-34.97	12.65
	$\delta^{18}\text{O}$	-22.25	-15.83	-11.88	-5.15	1.81
	lc-excess	-23.42	-4.78	10.9	-4.58	6.12
Tree 2 m	$\delta^2\text{H}$	-169.91	-120.14	-92.83	-35.7	13.14
	$\delta^{18}\text{O}$	-23.56	-15.94	-12.01	-5.25	1.87
	lc-excess	-24.63	-4.65	9.56	-4.34	6.07
Tree 10 m	$\delta^2\text{H}$	-170.32	-120.38	-89.67	-36.26	13.59
	$\delta^{18}\text{O}$	-23.48	-16.04	-11.84	-5.41	1.9
	lc-excess	-24.21	-4.15	8.7	-4.03	5.7